ROBUST CONTROLLER DESIGN FOR THE NUCLEAR REACTOR POWER BY EXTENDED FREQUENCY RESPONSE METHOD

YOON JOON LEE[1*] and MAN GYUN NA[2]
[1]Department of Nuclear and Energy Engineering, Cheju National University
Ara 1-dong, Cheju-City, 690-756, Korea
[2]Department of Nuclear Engineering, Chosun University
375 Seosuk-dong, Dong-gu, Gwangju 501-759, Korea
*Corresponding author. E-mail : leeyj@cheju.ac.kr

Received September 26, 2005
Accepted for Publication November 29, 2005

In this study, a controller for a nuclear reactor power is designed. The reactor is modeled using the three dimensional reactor design code MASTER. From the relationship of the input and output of the reactor code, a reactor dynamic model is derived by the system identification method. This model is more realistic than the one based on mathematical theories. With this model, a robust controller is designed by the extended frequency response method. As this method has the same theoretical background as the classical method, all of the existing design techniques of the classical method can be used directly. Furthermore, by introducing the real part of a Laplacian operator into the frequency response, the control design specification can be considered at the initial stage of design. The designed controller is simple, and gives a sufficient robustness with good performance.

KEYWORDS : Power Control, Nuclear Reactor, Robustness, Extended Frequency Response

1. INTRODUCTION

In the process of designing a control system, the most important consideration is to characterize the plant that is to be controlled. However, an exact modeling of a plant is, in reality, impossible. Plant modeling includes the linearization of non-linearities as well as approximations in the mathematical description. In addition, the designed system is apt to change because of varying operating conditions, set point drift, equipment aging and so on. The actual system should work as intended under real circumstances even if it is designed on the basis of an inexact model. This capability is defined as system robustness on which this study focuses.

There are numerous design methods for system robustness, ranging from classical loop shaping to the modern algorithm of the H-infinity method. Each has its own merits and drawbacks. For example, loop shaping is the foundation of nearly all control designs but it requires designer experience and is subject to the designer's discretion. The H-infinity theory is theoretically sound but it is mathematically involved and yields a high order controller, which presents difficulty in actual implementation [1].

At present, many modern control algorithms have been developed. Some examples are the optimal control, neural, model predictive control, and parametric approaches by the polynomial theory [2,3]. Several of these methods are based on dynamically varying plant models, and some are achieved by considering only the measured input and output data. However, although the modern controllers are successful in particular areas, most automatic control systems for complex non-linear, non-stationary objects in process industries are performed by typical P and PI algorithms. Their performance and reliability have been proven in various fields of application over an extended period. These classical algorithms are widespread because of their tuning simplicity, sufficient dynamic accuracy, and robustness.

The design object for a classical controller is to determine the control parameters. This is usually achieved through a frequency response analysis. However, contrary to a lead or lag controller, it is difficult to determine the optimal set of control parameters; hence an empirical method such as Ziegler-Nichols is used to determine the parameter values. A frequency response analysis is the control design method in the frequency domain that is obtained by mapping the Laplacian domain with the relationship of $s = j\omega$. However, by using the relationship of $s = real + imaginary$, the control design specification can be considered in the initial stage of the design. And by applying the design specification

in the initial design stage, the trial and error process that is usually encountered in control system designs can be reduced.

The control system design starts from a mathematical description of the process. Usually, it is impossible to obtain an exact model. However, a more stable and efficient control system is obtained with a more exact model. A requirement for all control systems is to solve and to cope with system uncertainties. The uncertainty of the plant depends on the actual system. For mechanical and electrical systems, the uncertainty is often comparatively small, as the system can be defined with a small error. On the other hand a nuclear reactor has a large uncertainty, as the main mechanisms of the nuclear reactor are thermal-hydraulic and nuclear. These mechanisms have various uncertainties originating from the material properties and the geometrical charateristics and operating conditions. Thus they are difficult to describe with a set of mathematical equations.

This paper consists of two parts. First, the nuclear reactor model was determined using the 3D reactor design code MASTER [4]. Following this, a PID controller was developed by an extended frequency method.

2. DYNAMIC REACTOR MODEL

A reactor model can be obtained mathematically from the nuclear kinetic equations and thermal hydraulic energy balance equations. These equations are, however, much too simple to describe an actual reactor. As an alternative, a reactor model can be derived from the relationship of the input and output of the reactor. The reactor powers for the control rod movements for the reactors Yonggwang 3 & 4 are obtained by the three dimensional reactor design code MASTER, and the system identification method is applied to the input-output relationship to describe the reactor with a linear model. This approach takes account of all realistic conditions, and the reactor model determined by this method is more realistic than the model derived from theoretical descriptions.

To describe a more realistic situation, the overlapping scheme and insertion limits of Yonggwang 3 & 4 (PWR, 1000MW $\times$ 2) are taken into consideration [5]. The control rods are driven by two error signals. They are the power mismatch between turbine and reactor, and the coolant temperature deviation from the reference temperature. These signals are summed and input to the rod speed programmer to drive the rods. This scheme is nearly identical to schemes in other plants. The reactor has five regulating control banks (R5, R4, R3, R2 and R1) to control the power level and two partial-strength control banks (P1 and P2) to regulate the axial power distribution. The leading insertion bank of the regulating control banks is R5. The other banks are inserted in order of R4, R3, R2 and R1 with an overlap of 229 steps. This overlap makes the radial flux distribution more even, and produces the linear integral rod worth.

The movements of control rod bank R5 are used as the input to the reactor. The other bank, R4, moves together with R5 in compliance with the scheduled overlapping mode. Therefore, an actual situation is obtained although the input to the reactor is described by R5 only.

The initial rod positions of R5 are changed in increments of 25 steps from the fully inserted position of 0 steps to 152 steps (7 cases), and in increments of 50 steps from 152 steps to the fully withdrawn position of 381 steps (5 cases), for a given power level. The positions of R4 are considered. For example, when the position of R5 is 50 steps, the position of R4 is 279 steps, and with R5 at 152 steps or more, R4 is in the fully withdrawn state. 12 cases of the rod positions are considered for a given initial power, and 11 initial powers from 0% to 100% in increments of 10% are considered. Hence, 132 cases are tried in order to describe the reactor in terms of the initial steady state power and the initial rod position. The dynamic run of MASTER

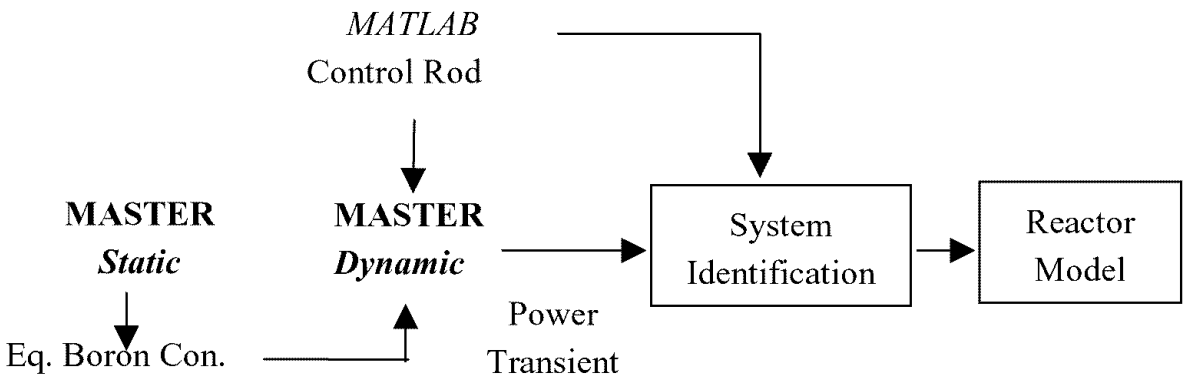

Fig. 1. Procedure of Obtaining a Reactor Model

requires an equilibrium boron concentration of the initial steady state, and this boron concentration is obtained from a static run of MASTER.

Figure 1 shows the overall modeling procedure. The equilibrium boron concentration for a given initial power and rod position is determined by a static MASTER run, and is used for the dynamic MASTER run. The long-term dynamics of the fuel burn-up is not considered, and equilibrium states of poisons are assumed. The input to MASTER is the movement of control rod bank R5, overlapped with R4. As the system identification requires sufficiently varying inputs, the rod movement is described by another utility of MATLAB, which is linked with MASTER. All of the physical data used in the code are from Yonggwang Units 3 & 4 [5].

Simulations are made for total 132 cases for various initial powers and initial rod conditions. The sampling period is three seconds. For a given case, with the input data of the control rod movement and the output data of the power transients, the system identification is made using an autoregressive exogenous algorithm and its variations [6,7]. The reactor plant is described both by a 4th order and by a 5th order transfer function in the z-domain.

$$G(z)_{4th} = \frac{n_1 z^3 + n_2 z^2 + n_3 z + n_4}{d_0 z^4 + d_1 z^3 + d_2 z^2 + d_3 z + d_4}, \qquad G(z)_{5th} = \frac{n_1 z^4 + \mathrm{L} + n_4 z + n_5}{d_0 z^5 + \mathrm{L} + d_4 z + d_5} \tag{1}$$

In the above equation, the coefficients of the numerator and the denominator are different for each case. They are dependent both on the initial powers and on the initial rod positions. For example, Fig. 2 shows that the coefficient n_1 of the numerator for the 4th order system depends on the powers and rod speeds. Some irregularities are shown in Fig. 2(a). These are due to the rod overlapping, which is explained further by Fig. 2(b).

To describe the coefficients of the transfer function in terms of the initial steady state power level and initial rod position, a two-dimensional interpolation is used. That is, for a specific coefficient, a two-dimensional table of power and rod position is made, and the coefficient is found by the interpolation for a given power and rod position.

For an example, when the initial power is 65%, and the initial positions of R5 and R4 are 110 steps and 339 steps, respectively, the transfer functions are found to be

$$G(z)_{4th} = \frac{0.173 z^3 - 0.02633 z^2 - 0.02166 z - 0.01882}{z^4 - 0.1488 z^3 - 0.1214 z^2 - 0.1081 z - 0.0012} \tag{2}$$

$$G(z)_{5th} = \frac{0.1729 z^4 - 0.0262 z^3 - 0.0193 z^2 - 0.0199 z - 0.0118}{z^5 - 0.1487 z^4 - 0.1083 z^3 - 0.1144 z^2 - 0.0661 z + 0.0012} \tag{3}$$

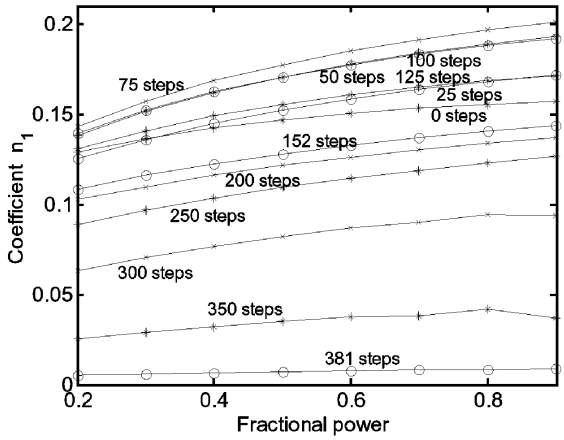

(a) Value of Coefficient n_1 by Initial Power Level

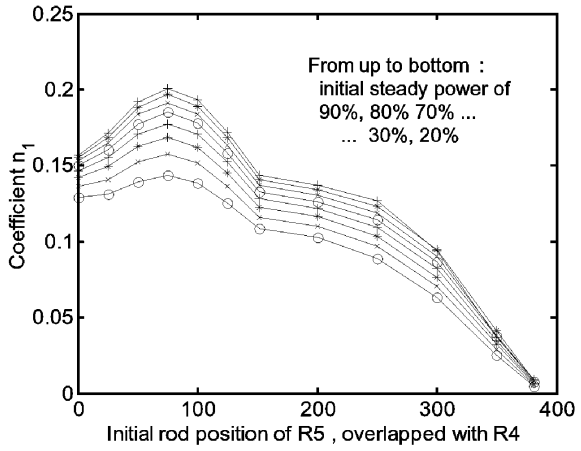

(b) Value of Coefficient n_1 by Rod Position

Fig. 2. Dependency of Transfer Function Coefficients on Power and Rod Position

3. CONTROLLER DESIGN BY EFR

In the EFR (Extended Frequency Response) method [8], the system is mapped into the extended frequency domain by the relationship of $s=-m\omega+j\omega$. In this case, the plant is then described by $G(m,\omega)$, instead of $G(\omega)$, in the conventional frequency domain. The value m can be regarded as a design specification. For the case of an impulse response

of a second system, the fading factor is found to be

$$\Psi = 1 - e^{-2\pi m} \equiv 1 - \frac{A_2}{A_1} \tag{4}$$

where, A_1 and A_2 are the amplitude of the first peak and the second peak, respectively.

For the case of the step response, the peak A_p, and the settling value A_s, of the amplitude have the relationship

$$A_p = A_s + exp(-\pi \cdot m) \tag{5}$$

Therefore, the design specification can be considered at the initial stage of the design. This is similar to the concept of pole location techniques in a state space, and it reduces the trial and error process in the design process.

The critical frequencies for the design of P, PI and PID should be known for the design. By defining

$$\psi_\mu(m,\omega) = tan^{-1}\left(\frac{I_\mu(m,\omega)}{R_\mu(m,\omega)}\right) + c(\omega), \quad R_\mu(m,\omega) = Real\left[G(m,\omega)\right],$$

$I_\mu(m,\omega) = Image\left[G(m,\omega)\right]$, where $c(\omega)=0$ for $R_\mu(m,\omega)>0$, otherwise $-\pi$, the critical frequency for the P and PI controllers is the frequency which satisfies $\psi_\mu(m,\omega)=-\pi$, and the PID critical frequency is obtained from $\psi_\mu(m,\omega)=\frac{-3\pi}{2}$. For reference, although the I controller is rarely used, the critical frequency is obtained from $tan^{-1}\left(\frac{I_\mu(m,\omega)}{R_\mu(m,\omega)}\right) + tan^{-1}\left(\frac{1}{m}\right) = 0$.

The reactor plant for the design is determined by assuming an initial power of 80%, and initial rod positions of R5 of 100 steps, overlapping with R4. The plant is then described with a 4th order equation, as

$$G(z) = \frac{0.1892z^3 - 0.03735z^2 - 0.03268z - 0.03169}{z^4 - 0.1976z^3 - 0.1727z^2 - 0.1688z - 0.0008} \tag{6}$$

This system is converted from the z-domain to the s-domain with a sampling period of three seconds, and the model order is increased to handle the real negative pole. The resulting continuous reactor model is

$$G_1(s) = \frac{0.3348s^4 + 1.003s^3 + 0.6901s^2 + 0.5314s + 0.04769}{s^5 + 4.165s^4 + 7.042s^3 + 4.872s^2 + 2.927s + 0.2509} \tag{7}$$

The plant of Eq. (6) is intrinsically stable. Additionally, for the purpose of considering an actual situation of an actuator delay and other disturbances, a delay of two seconds is applied in the form of Pade. The reactor plant for which the controllers are designed is then

$$G(s) = G_1(s) \cdot D(s), \; D(s) = \frac{s^2 - 3s + 1}{s^2 + 3s + 1} \tag{8}$$

In the EFR domain, the plant of Eq. (8) is

$$G(m,\omega) = G_1(m,\omega) \cdot D(m,\omega)$$

$$G_1(m,\omega) = \frac{0.3348 \cdot (-m\omega + j\omega)^4 + 1.003 \cdot (-m\omega + j\omega)^3 \ldots + 0.04769}{(-m\omega + j\omega)^5 + 4.165 \cdot (-m\omega + j\omega)^4 \ldots + 2.927 \cdot (-m\omega + j\omega) + 0.2509},$$

$$D(m,\omega) = \frac{(-m\omega + j\omega)^2 - 3 \cdot (-m\omega + j\omega) + 1}{(-m\omega + j\omega)^2 + 3 \cdot (-m\omega + j\omega) + 1} \tag{9}$$

3.1 Proportional Controller

The characteristic equation of the system is $1+G(m,\omega)\,C(m,\omega)=0$, and as the controller is the gain only, $C(m,\omega)=K_P$. Therefore, the proportional controller is obtained from

$$K_P = \frac{1}{\left|G(m,\omega_P)\right|} \tag{10}$$

where ω_P is the critical frequency.

The design specification of Eq. (10) is the value of m. Figure 3 shows the system responses for various values of m.

As shown in the figure, as the m-value becomes smaller, the gain becomes larger, which results in the larger fluctuation. Hence, by considering the system speed and stability, the design specification of the m-value is determined as 0.366. In this case, the proportional controller is

$$K_P = \frac{1}{\left|G(m,\omega_P)\right|} = \frac{1}{\left|G(0.366,1.255)\right|} = 2.0964 \tag{11}$$

Although the proportional controller is the simplest controller, the settling values are different for different gains, and an additional gain is necessary to make the system output follow the command input.

3.2 Proportional-Integral Controller

The PI controller is $C(s) = K_P + \frac{K_I}{s} = K_P + \frac{K_P}{T_I s}$, or $C(m,\omega) = K_P + \frac{K_I}{-m\omega + j\omega}$. From the characteristic equation

condition of $1+G(m,\omega)C(m,\omega)=0$, $Real[G(m,\omega)C(m,\omega)]=-1$ and $Image[G(m,\omega)C(m,\omega)]=0$. By letting $Real[G(m,\omega)]=R_\mu(m,\omega)$ and $Image[G(m,\omega)]=I_\mu(m,\omega)$, K_P and K_I are found to be

$$K_P(m,\omega)=\frac{-R_\mu(m,\omega)-mI_\mu(m,\omega)}{R_\mu(m,\omega)^2+I_\mu(m,\omega)^2} \tag{12}$$

$$K_I(m,\omega)=\frac{-\omega(1+m^2)I_\mu(m,\omega)}{R_\mu(m,\omega)^2+I_\mu(m,\omega)^2}, \quad K_I=0, \text{ if } K_I(m,\omega)<0 \tag{13}$$

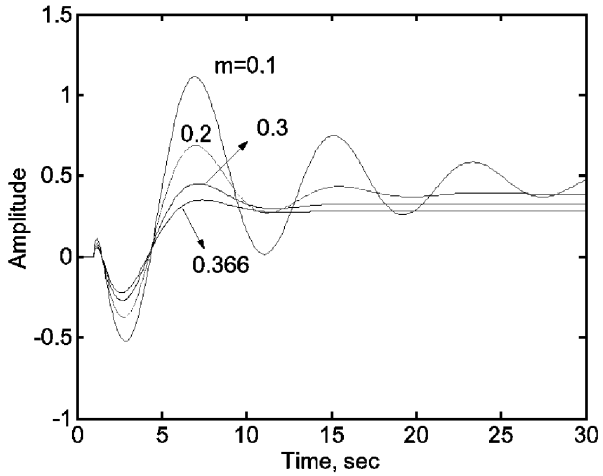

(a) System Responses for m =0.1 to 0.366

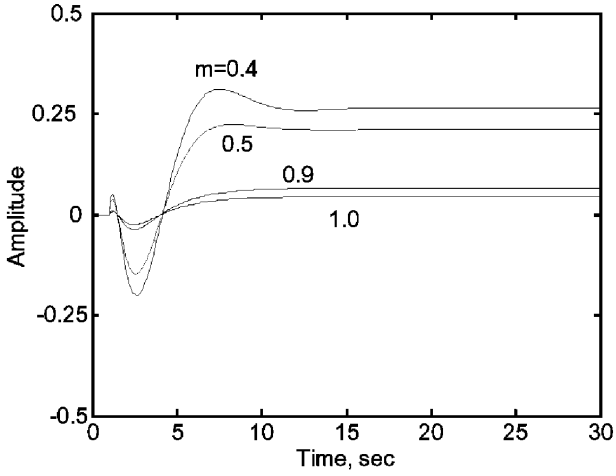

(b) System Responses for m =0.4 to 1.0

Fig. 3. System Responses with Proportional Controller for Various m-Values

The design specification is the value of m, as in the case of proportional controller. The controller parameters, K_P and K_I, are calculated for several values of m; they are shown in Fig. 4.

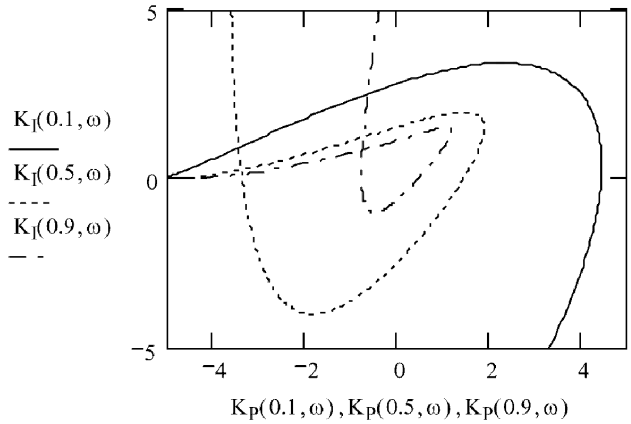

Fig. 4. Control Parameters for Various Values of m

As shown in Fig. 4, the ranges of K_P and K_I shrink with an increasing value of m. This is as expected, because a large value of m indicates that the system is fully damped. That is, the system response is somewhat slower but the stability margin is large. With a consideration of both performance and stability, an m value of 0.5 is used in the design of the PI controller.

Figure 5 describes the values of K_P and K_I as a function of frequency. The frequency to be used in the determination of $K_P(m,\omega)$ and $K_I(m,\omega)$ is calculated from

$$\frac{dK_I(m,\omega)}{d\omega}=\frac{dK_I(0.5,\omega)}{d\omega}=0 \tag{14}$$

The frequency that satisfies this condition is ω= 0.7086, and from Eq. (13), the parameters are found to be $K_P(m,\omega)$ =1.966 and $K_I(m,\omega)$=0.842.

With this PI controller, the gain margin is 8.75dB at ω= 1.1795 rad/sec, and the phase margin is 87.8 degrees at ω= 0.1709 rad/sec. This margin is sufficiently large for system stability.

The time responses for the step change of the system are presented in Figs. 6(a) and (b) for the system output and the control input, respectively. The system settles to the steady state value with a rapid speed, and the overshooting is not great.

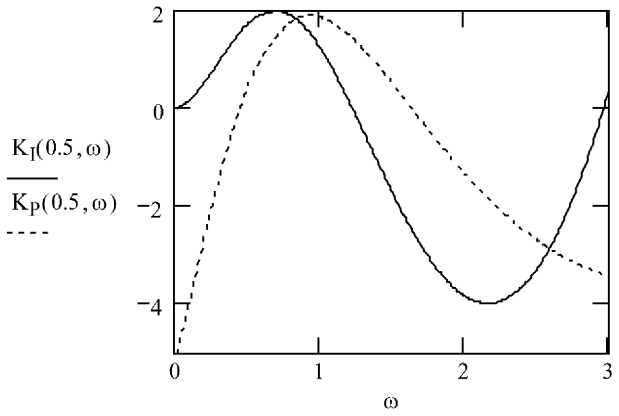

Fig. 5. K_P and K_I vs. Frequency

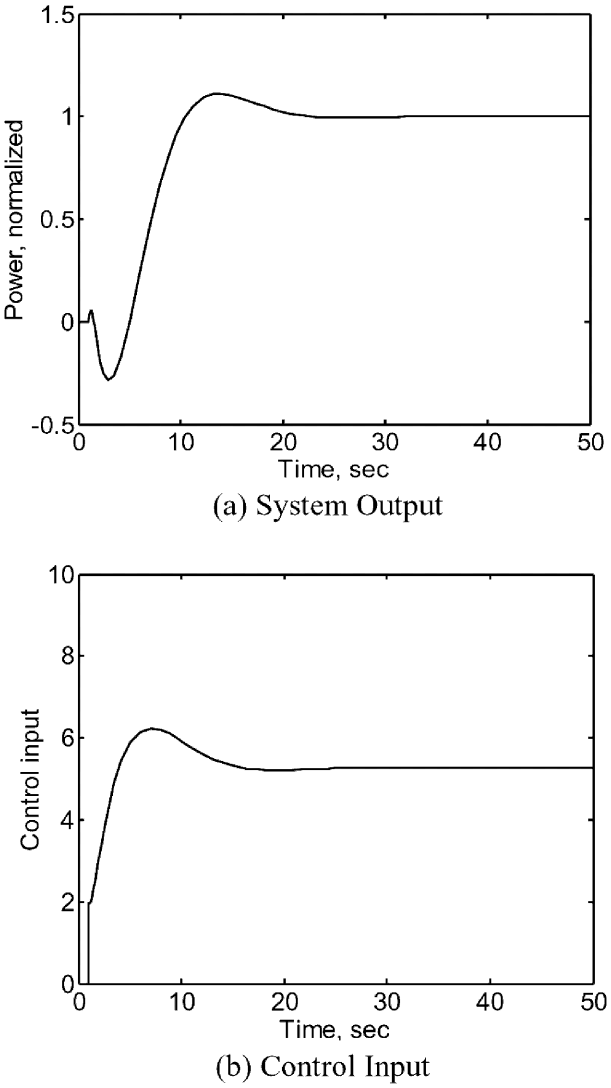

Fig. 6. System Responses with the PI Controller

3.3 Proportional-Integral-Derivative Controller

The PID controller is

$$C(s) = K_P\left(1+\frac{1}{T_i s}+T_d s\right) = K_P+\frac{K_I}{s}+\left(K_P\cdot\alpha\cdot T_i\cdot s\right), \quad K_I=\frac{K_P}{T_i}, \text{ and } \alpha=\frac{T_d}{T_i} \tag{15}$$

The unknowns are K_P, T_i and T_d. However, by regarding α as a design specification, the unknowns reduce to K_P and T_i, and they are functions of m, α and frequency. The physical implication of m is the system response speed. Similarly, the value of α is related to system performance and stability. The primary reason for the integral control is to eliminate the steady state error, but this typically comes at the cost of reduced stability. Usually, any system becomes less stable or less damped by the addition of an integral control. Increasing the gain of K_P/T_i will ultimately result in lightly damped roots, which is equivalent to a small value of m. A derivative control is to increase the damping and generally to improve the stability of the system. In this regard, α links the effects of an integral and a derivative control. As the increasing $1/T_i$ reduces system stability, the large value of α indicates a less stable system and the small value of α denotes a more stable and robust system.

Similar to the PI design, the PID controller should satisfy the condition of the characteristic equation. Then,

$$Real\left[G(m,\omega)C(\alpha,m,\omega)\right]=-1, \quad Image\left[G(m,\omega)C(\alpha,m,\omega)\right]=0 \tag{16}$$

By letting the real and imaginary parts of the plant $G(m,\omega)$ be $R_\mu(m,\omega)$ and $I_\mu(m,\omega)$, respectively, the control parameters are found to be

$$T_i(\alpha,m,\omega)=\frac{-A_1(m,\omega)-\sqrt{A_1(m,\omega)^2-4A_2(\alpha,m,\omega)\cdot A_0(m,\omega)}}{2A_2(\alpha,m,\omega)} \tag{17}$$

where ,

$$A_0(m,\omega)=-\left(\frac{m\cdot I_\mu(m,\omega)+R_\mu(m,\omega)}{\omega\cdot(1+m^2)}\right),\ A_1(m,\omega)=I_\mu(m,\omega), \text{ and}$$

$$A_2(m,\omega)=R_\mu(m,\omega)\cdot\alpha\cdot\omega-I_\mu(m,\omega)\cdot\alpha\cdot\omega\cdot m \tag{18}$$

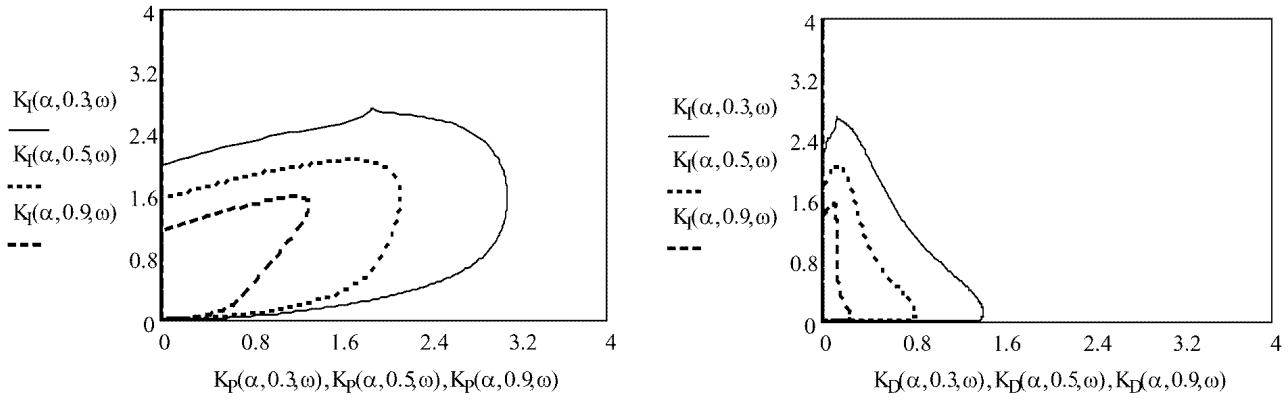

(a) α =0.1

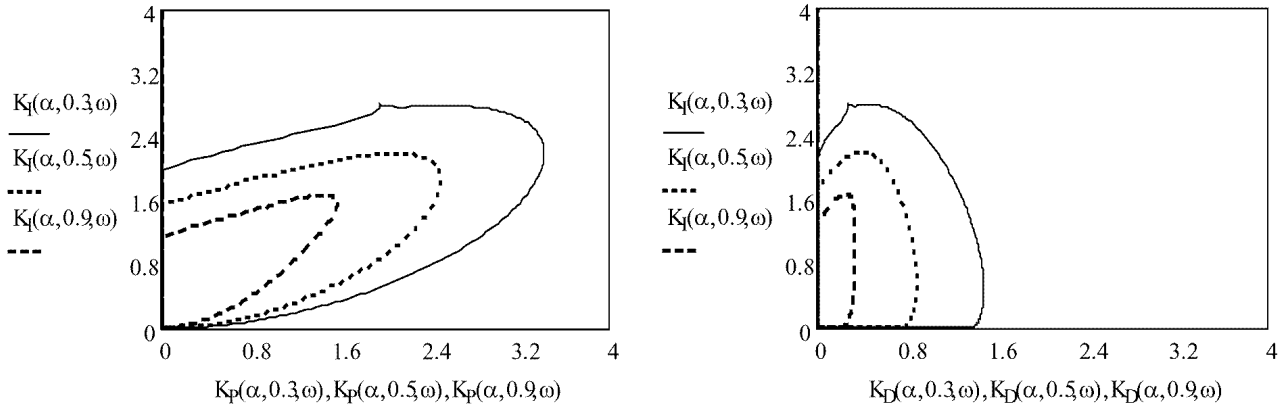

(b) α =0.2

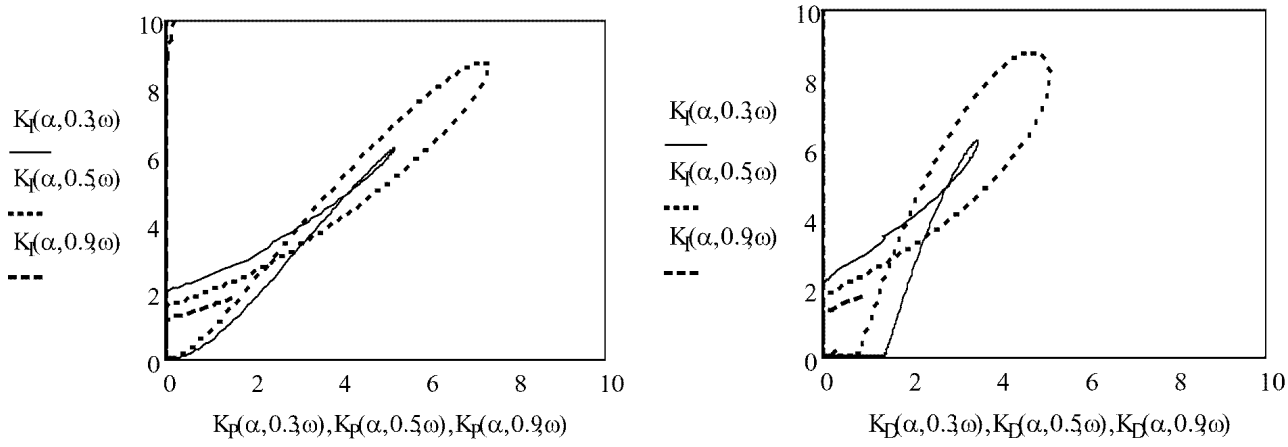

(c) α =0.8

Fig. 7. Ranges of Control Parameters for Different Values of α (m=0.3, 0.5 and 0.9)

and

$$K_i(\alpha,m,\omega)=\frac{1}{B(\alpha,m,\omega)+C(\alpha,m,\omega)} \tag{19}$$

where,

$$\begin{aligned}B(\alpha,m,\omega)=&\\ &\omega\cdot T_i(\alpha,m,\omega)^2\cdot\alpha\cdot\left(m\cdot R_\mu(m,\omega)+I_\mu(m,\omega)\right)\\ &-T_i(\alpha,m,\omega)\cdot R_\mu(m,\omega)\end{aligned}$$

$$C(\alpha,m,\omega)=\frac{m\cdot R_\mu(m,\omega)+I_\mu(m,\omega)}{\omega\cdot(1+m^2)} \tag{20}$$

$$K_P(\alpha,m,\omega)=K_I(\alpha,m,\omega)\cdot T_i(\alpha,m,\omega),\quad \text{if } K_P(\alpha,m,\omega)>0 \text{ otherwise } K_P(\alpha,m,\omega)=0 \tag{21}$$

$$K_D(\alpha,m,\omega)=\alpha\cdot K_P(\alpha,m,\omega)\cdot T_i(\alpha,m,\omega) \tag{22}$$

Figure 7 shows the calculated results for three α values of 0.1 (robust), 0.2 and 0.8 (fast). In each figure, the control parameters for three cases of $m=0.3$ (lightly damped), 0.5 and 0.9 (heavily damped) are compared to each other.

As shown in the figure, with the increase of the α value, the control parameters become large. The large value of α implies that the system is stable and robust, and large values of control parameters can be permitted. Furthermore, for a given value of α, the ranges of the control parameters are different depending on the m value. A small value of m indicates that the system is lightly damped and is less stable. For example, when α is 0.1 (Fig. 7a), the control parameter range shrinks with the increase of m, which makes the system more stable, but at a cost of poorer performance. However, this trend becomes different when α reaches a certain value. When α is approximately 0.6, the control parameter range for $m=0.5$ exceeds that for $m=0.3$. This trend becomes more significant with the increase of α. This can be interpreted as follows: When α is small, the system is stable and the increase of m yields more damping, resulting in small control parameter ranges. In contrast, when α is large, the system becomes unstable, and a large value of m is required for stability, resulting in large control parameter ranges. Considering these findings, the α value of 0.2 was chosen for the design specification to assure system stability.

The control parameters depend on frequencies. The same frequency should be applied to the determination of control parameter values. The frequency that makes the proportional gain maximum is different from the frequency that makes the integrator gain maximum. Usually, if ω_P, the frequency at which the proportional gain is the maximum, is used, the fluctuation of the system becomes large. If ω_I is used, the integrated gain becomes so large as to make the system unstable and in some cases, the system diverges. If ω_D is used, the maximum derivative gain value makes the system stable, and at this frequency the integrator gain is usually small, which leads to a more stable system. Hence ω_D is used in the design of the PID controller.

Three cases are investigated. They are m=0.2, 0.5 and 0.8. The α value is fixed as 0.2, as explained above. For each case, ω_D is determined from $\frac{dK_D(0.2,m,\omega)}{d\omega}=0$; the control parameters are summarized in Table 1.

Table 1. Control Parameters of PID

Case	α	m	ω_D	K_P	K_I	K_D
A	0.2	0.2	1.942	1.944	0.394	1.917
B	0.2	0.5	1.581	1.59	0.571	0.886
C	0.2	0.8	1.246	1.116	0.597	0.417

The Bode diagrams show that Case A has too much margin, resulting in a sluggish output. Cases B and C give the nearly identical results with better performance. Figure 8 describes the system responses for Case B. The system speeds are relatively fast, and the over-shoots are negligible. The initial decreases in system output are due to the delay, which makes the system a non-minimum phase system.

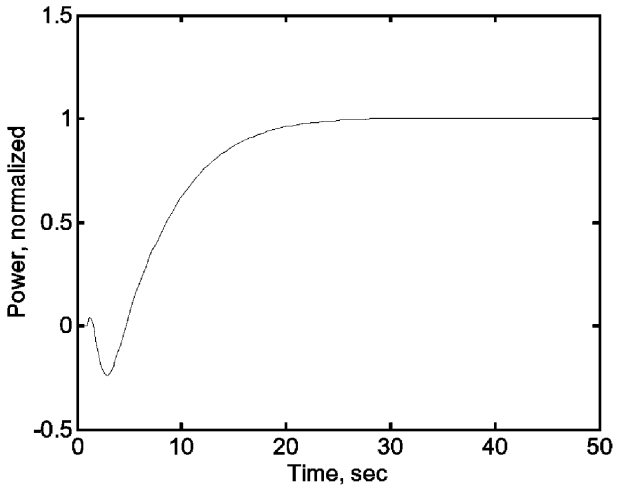

(a) System Output

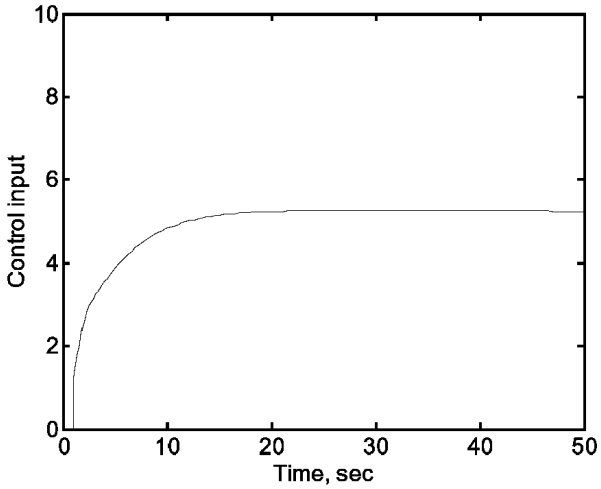

(b) Control Input

Fig. 8. System Responses with PID, m=0.5, K_P=1.59, K_I=0.571, K_D=0.886

The PID controllers explained above are designed based on the plant at 80% initial power with an R5 position of 100 steps. However, the transfer function of the plant becomes different with changes of the initial conditions of the plant. To verify the robustness of the designed PID controller, simulations are made for two cases. The first case is for an initial power of 80%, and the initial rod positions are assumed to be 150 steps and 50 steps. The second is with an initial rod position of 100 steps, and the initial powers are assumed as 90% and 50%. The same PID of K_P=1.59, K_I=0.571, K_D=0.886 is applied to each case.

It was found that the system responses are similar in each case. This indicates that although there is a disturbance in the plant, or the plant becomes different depending on the operating conditions, the designed PID maintains the system performance and stability, which suggests that the designed PID guarantees the system robustness.

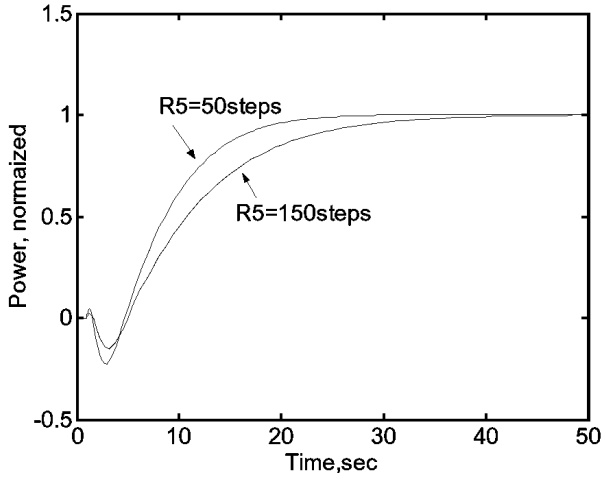

(a) Plants with Different Initial Rod Positions

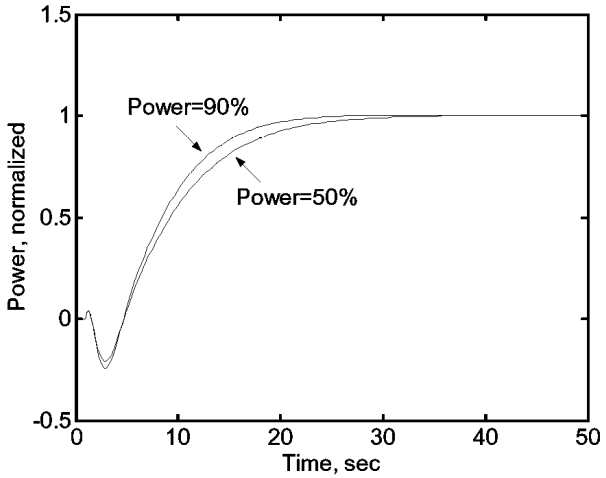

(b) Plants with Different Initial Powers

Fig. 9. Responses of the System for Different Initial Conditions of the Plant

4. SUMMARY AND CONCLUSIONS

The reactor powers for the control rod movements for the reactor of Yonggwang 3 & 4 are obtained through a simulation using the three-dimensional reactor design code, MASTER and the system identification method is applied to the input-output relationship in order to describe the reactor by a linear model. The simulation takes accounts of realistic conditions such as rod overlapping, and the reactor model determined by this method is more realistic than the model derived from the theoretical descriptions. However, this model is not exact, and the control system should have a sufficient robustness for the actual system to work as intended under real circumstances.

There are numerous design methods for system robustness ranging from classical loop shaping to the modern algorithm of the H-infinity method. However, most of the automatic control systems of complex non-linear, non-stationary objects in actual industry processes are performed by typical P and PI algorithms. These classical algorithms are widely used due to their tuning simplicity, sufficient dynamic accuracy and robustness.

The most complicated practical algorithm is the PID algorithm. The PID algorithm is similar to the optimal Wiener algorithm for a control system that has no lag and low frequency disturbances. Although it enhances dynamic accuracy, it is not as widely used as the P and PI algorithms.

The main reasons for the restricted use of the PID algorithm are its tuning complicity and high sensitivity to variations in system parameters. However, by introducing the real part of the Laplacian operator into the frequency response domain, the determination of the control parameters can be made in a more systematic manner. The system stability and performance depend on the pole locations, and these locations can be considered easily at the initial design stage in the EFR.

Three controllers of P, PI and PID were designed by the EFR method. The designed controllers provide the system with good performance and stability. Even with wide plant changes, the system output shows a similar pattern, which demonstrates good robustness.

REFERENCES

[1] Y. J. Lee, "H_∞ Robust Controller Design of Reactor Power Control System," *J. of KNS*, Vol. **29**(4), pp. 280-290 (1997).

[2] M. G. Na, Y. R. Sim, Y. J. Lee, "Design of an Adaptive Predictive Controller for Steam Generators," *IEEE Trans. on Nuc. Sci.*, Vol. **90**(1), pp. 186-193 (2003).

[3] Y. J. Lee, M. G. Na, "Robust Controller Design of Nuclear Power Reactor by Parametric Method," *J. of KNS*, **34**(5). pp. 436-444, Oct., 2002.

[4] "MASTER (Multi-purpose Analyzer for Static and Transient Effects of Reactors)," ver. 2.1, KAERI/UM-06/2000 (2000).

[5] *Final Safety Analysis Report of Yonggwang Unit 3 & 4*, Korea Electric Power Corp. (1992).

[6] *L. Ljung, System Identification*, 2nd ed., 8-12, Prentice Hall (1999).

[7] K. J. Astrom, B. Wittenmark, *Adaptive Control*, 75-76, Addison Wesley (1989).

[8] V. V. Volgin, O. C. Kharitonova, "The Selection of Robust Tuning of PID Regulating Algorithms," *Procd. Control 2003*, MPEI, Moscow, Russia Oct. 22- 24, 2003.